A STUDY OF WIDE BAND $Zn_{1-x}Mg_xO$ AND $(Ga_xIn_{1-x})_2O_3$ THIN FILMS PREPARED BY THE SPIN COATING METHOD

Vadim Morari[1*], Veaceslav Ursaki[2,3], Lidia Ghimpu[1], Emil Rusu[1], and Ion Tiginyanu[2,3]

[1]Ghitu Institute of Electronic Engineering and Nanotechnologies, Chisinau, MD-2028 Republic of Moldova
[2]National Center for Materials Study and Testing, Technical University of Moldova, Chisinau, MD-2004 Republic of Moldova
[3]Academy of Sciences of Moldova, Chisinau, MD-2001 Republic of Moldova.
**E-mail:vadimmorari2018@gmail.com*

https://doi.org/10.53081/mjps.2022.21-1.02

Abstract

This study presents a brief analysis of $Zn_{1-x}Mg_xO$ and $(Ga_xIn_{1-x})_2O_3$ thin films deposited on Si substrates by the spin coating method. The morphology and chemical composition of the prepared thin films were studied by scanning electron microscopy (SEM) and energy dispersive X-ray (EDX) analysis. The evolution of the crystal structure with a change in the film composition and the technological conditions for annealing after spin coating was studied by X-ray diffraction (XRD) analysis. The annealing atmosphere and temperature were optimized in terms of producing films with a stoichiometric composition and a high crystalline quality.

Keywords: thin films, SEM, EDX, XRD, spin coating, stoichiometry, crystal structure.

Rezumat

Acest studiu prezintă o scurtă analiză a filmelor subțiri de $Zn_{1-x}Mg_xO$ și $(Ga_xIn_{1-x})_2O_3$ depuse pe substraturi de Si prin metoda spin coating. Morfologia și compoziția chimică a filmelor subțiri obținute au fost studiate prin microscopie electronică cu scanare (SEM) și analiză cu raze X cu dispersie de energie (EDX). Evoluția structurii cristaline odată cu modificarea compoziției filmului și a condițiilor tehnologice de recoacere după depunerea prin metoda spin coating, a fost investigată prin analiza de difracție cu raze X (XRD). Atmosfera de recoacere și temperatura au fost optimizate din punct de vedere al obținerii filmelor cu compoziție stoichimetrică și structură cristalină de calitate înaltă.

Cuvinte cheie: filme subțiri, SEM, EDX, XRD, spin coating, stoichiometrie, structură cristalină.

1. Introduction

In the last years, a lot of emphasis has been placed on wide band gap optoelectronic devices, particularly those based on SnO_2 films with high electrical conductivity properties combined with excellent transparency and thermal stability [1, 2]. Tin oxide SnO_2, being a wide

band gap semiconductor, has a band gap of 3.6 eV at room temperature. At the same time, indium tin oxide (ITO) with the band gap in a range of 3.5–4.3 eV is also a thoroughly studied material due to its high conductivity and optical transparency [3]. Zinc oxide (ZnO) with a band gap of 3.4 eV is also used in optoelectronic devices due to its advantages over gallium nitride (GaN) in terms of technological aspects [4]. Thin films of zinc oxide with different Mg concentrations in the precursor solutions for obtaining a $Zn_{1-x}Mg_xO$ solid solution offer the possibility of modeling the optical, luminescent, and photoelectric properties in a fairly wide range to reach a band gap of up to 7.8 eV [5–8]. Typically, these thin films are prepared by atomic layer deposition [9, 10], molecular beam epitaxy [11, 12], pulsed laser deposition [13, 14], and magneton sputtering [15]. Thin films of $(Ga_xIn_{1-x})_2O_3$ represent another attractive oxide semiconductor due to possibilities of tuning the material bandgap in a wide range of 3.5–5 eV by changing the alloy composition. In particular, this material system is promising for short-wavelength optical applications, such as solar-blind UV detectors [16–20]. Thin films of In_2O_3 and Ga_2O_3 have been previously obtained by different growth methods, such as metal-organic chemical vapor deposition (MOCVD) [21], halide vapor phase epitaxy (HVPE) [22], molecular beam epitaxy (MBE) [23], and pulsed laser deposition (PLD) [24]. Little attention has been given to films obtained by the spin coating method, despite the fact that it is one of the cheapest techniques. This paper presents a summary of our research on the change in film morphology using different annealing atmospheres for $Zn_{1-x}Mg_xO$ and the change in crystal structure depending on the Ga content for $(Ga_xIn_{1-x})_2O_3$ deposited on Si substrates by the spin coating method.

2. Sample Preparation Experimental Details

Solutions of zinc acetate ($Zn(CH_3CO_2)_2 \times 2H_2O$) and magnesium acetate ($Mg(CH_3COO)_2 \times 4H_2O$) (0.5 M) were dissolved in 2-methoxyethanol and diethanolamine (DEA), an organic compound with the formula $HN(CH_2CH_2OH)_2$ as a stabilizer, to obtain $Zn_{1-x}Mg_xO$ thin films by the spin coating method. The ZnO solutions with different Mg concentrations were mixed in an ultrasonic bath at a temperature of 50–60°C for 30 min. Spin coating was performed at room temperature on Si substrates in multiple coating cycles (5, 10, 15) at a rotational speed of 3000 rpm with 30-s rotation followed by drying the coated layer at 180°C for 10 min. After depositing a number of layers, which determine film thickness, some samples were analyzed by SEM and EDX without heat treatment, while other samples were analyzed after annealing in air and an argon atmosphere at a temperature of 500°C for 1 h.

For the deposition of $(Ga_xIn_{1-x})_2O_3$ thin films on Si substrates by the spin coating method, solutions of indium chloride ($InCl_3$) and gallium nitrate ($Ga(NO_3)_2$) (0.5M) were dissolved in 2-methoxyethanol and DEA as a stabilizer. The In_2O_3solutions with different Ga concentrations were mixed in an ultrasonic bath at a temperature of 50–60°C during 30 min before the deposition process. Spin coating was performed at room temperature on Si substrates in five coating cycles at a rotational speed of 3000 rpm with 30-s rotation followed by drying the coated layer at 180°C for 10 min. Similarly to $Zn_{1-x}Mg_xO$ films, after depositing a number of layers, the samples were treated at a temperature of 500°C in air for 1 h.

The morphology and chemical composition of the prepared films were studied by scanning electron microscopy (SEM) on a FEI Helios Nanolab 600 (SEM/FIB) combined instrument with a gallium focused ion beam equipped with a built-in X-ray detector with a sensor area of 30 mm^2 (Ametek, model ELECT PLUS) for energy dispersive X-ray (EDX) analysis. Analysis of the crystal structure and phases content in the thin films was performed using a Bruker AXS D8

DISCOVER X-ray diffractometer using monochromatic Cu$K_{\alpha 1}$ radiation (λ = 0.15406 Å) operating at a 40-kV beam voltage and a 40-mA beam current. Diffraction pattern data were collected for 2θ diffraction angles of 20°–80°.

3. Characterization of the Prepared Thin Films

One of the most thoroughly studied oxide semiconductor films is ZnO, which has a high exciton binding energy of 60 meV, which makes the excitons stable even at room temperature. The band gap of the material can be controlled by adding Mg in a certain concentration into the precursor solution of ZnO films to shift the spectral range of sensitivity to shorter wavelengths. Figure 1 shows the morphology of $Zn_{0.8}Mg_{0.2}O$/Si thin films prepared by the spin coating method and annealed in the different atmospheres at 500°C.

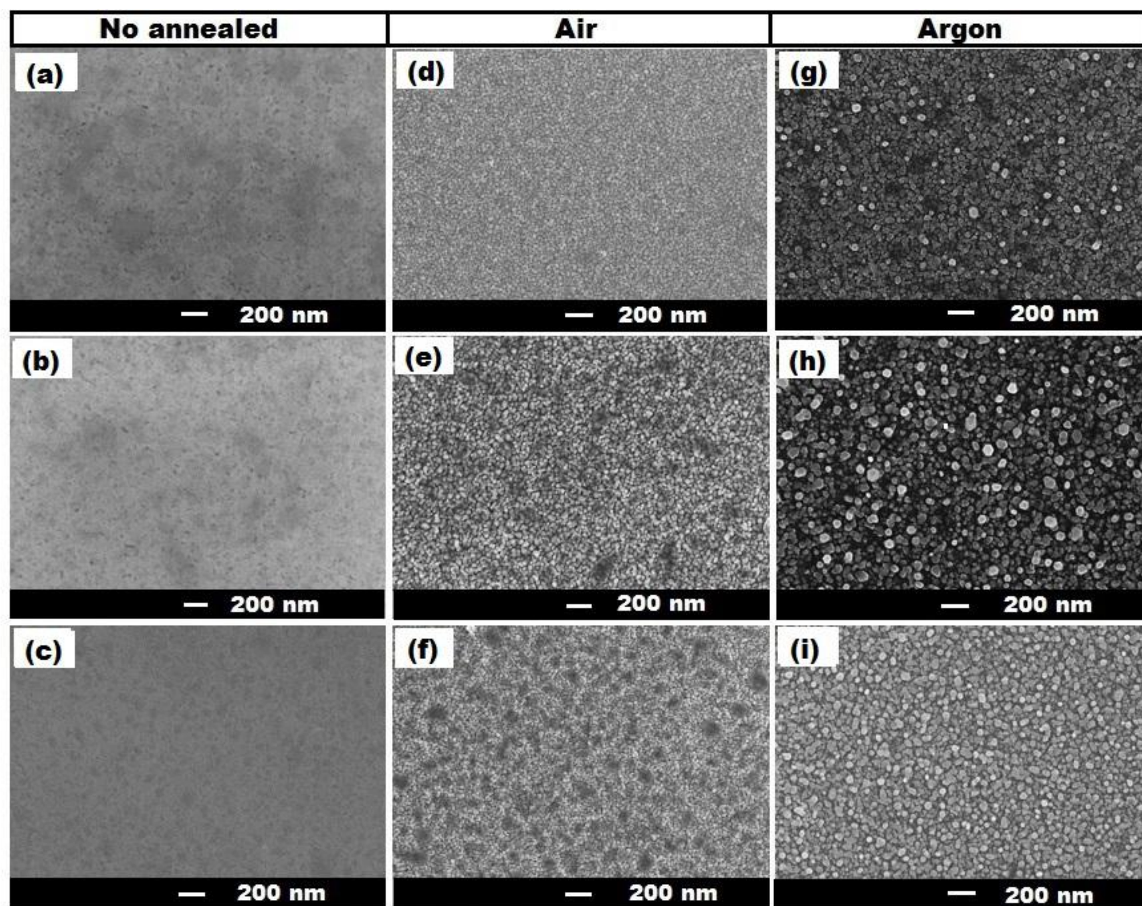

Fig. 1. Scanning electron microscopy images: top view of $Zn_{0.8}Mg_{0.2}O$/Si thin films prepared by the spin coating method and annealed in the different atmospheres: the first column shows samples with 15, 10, and 5 layers without annealing (a–c); the second column shows samples with 15, 10, and 5 layers, which were annealed in air (d–f); the third column shows samples with 15, 10, and 5 layers, which were annealed in argon (g–i).

It is evident from the images that the films without annealing are amorphous and do not contain any nanograins, regardless of their thickness (Figs. 1a–1c). In the case of annealing in air, nanograins are evident (Figs. 1d–1f). Annealing in argon shows the best results in terms of

nanograin size and quality (Figs. 1g–1i). The largest nanograins are detected in the samples with 10 deposited layers (Figs. 1e, 1h), which were annealed in air or argon; the crystallite size in them is about 20 and 50 nm, respectively.

Figure 2 summarizes the dependence of film thickness on the number of deposition cycles for $Zn_{0.8}Mg_{0.2}O/Si$ thin films prepared by the spin coating method and annealed in the different atmospheres. It is evident that the film thickness increases with an increase in the number of layers. The film thickness increases from 50 to 90 and 155 nm with an increase in the number of deposited layers from 5 to 10 and 15, respectively. Analysis of the results suggests that the film composition is non-stoichiometric, especially for the non-annealed films. This fact can be attributed to a large amount of carbon coming from the organic compound used as a precursor. However, the stoichiometry is improved after annealing due to a decrease in the amount of carbon. The samples treated in argon at 500°C are closer to stoichiometry; the best result in terms of stoichiometry and morphology is achieved for the 10-layer sample. Table 1 shows results of EDX analysis of $Zn_{0.8}Mg_{0.2}O$ thin films with different thicknesses prepared by the spin coating method and annealed in the different atmospheres.

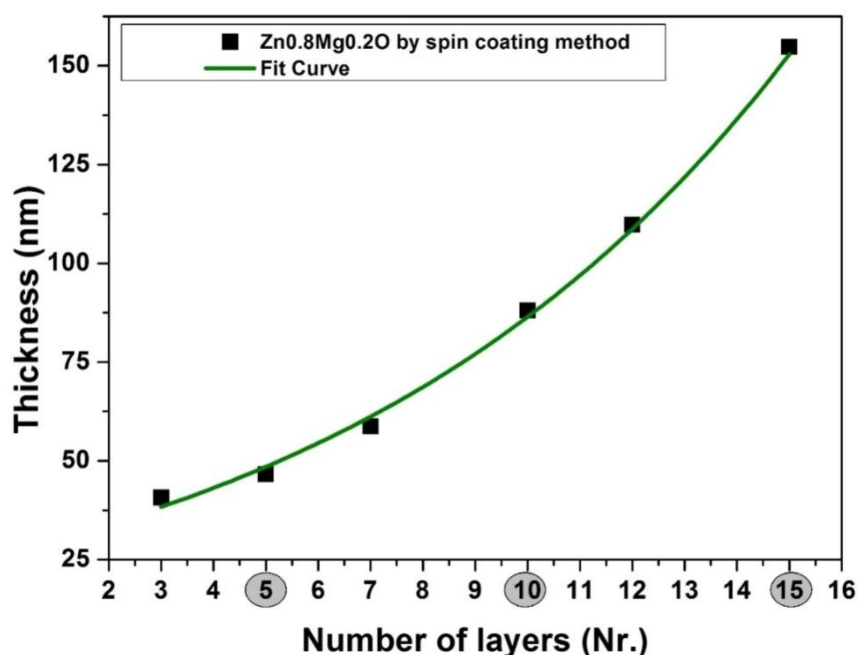

Fig. 2. Dependence of film thickness on the number of deposition cycles for $Zn_{0.8}Mg_{0.2}O/Si$ thin films prepared by the spin coating method and annealed in an argon atmosphere.

The XRD analysis (Fig. 3) revealed a single-phase wurtzite structure of the $Zn_{0.8}Mg_{0.2}O$ thin film [5, 25]. The non-annealed films are amorphous. Reflections from the wurtzite phase of the ZnMgO films (PDF card no. 01-078-3032) appear after annealing in air, while the best crystalline quality is obtained in the case of annealing in an argon atmosphere, as evidenced by the higher intensity of XRD reflections.

Table 1. Results of EDX analysis of $Zn_{0.8}Mg_{0.2}O$ thin films with different thicknesses prepared by the spin coating method and annealed in the different atmospheres

	No annealed			Air			Argon		
	Elements	Weight %	Atomic %	Elements	Weight %	Atomic %	Elements	Weight %	Atomic %
15 – layers	Mg	39.89	28.52	Mg	47.49	25.68	Mg	42.90	22.91
	Zn	60.11	71.48	Zn	52.51	74.32	Zn	57.10	77.09
	Total	100.00	100.00	Total	100.00	100.00	Total	100.00	100.00
10 – layers	Elements	Weight %	Atomic %	Elements	Weight %	Atomic %	Elements	Weight %	Atomic %
	Mg	41.63	31.22	Mg	35.30	27.23	Mg	42.53	23.50
	Zn	58.37	68.78	Zn	64.70	72.77	Zn	57.47	76.50
	Total	100.00	100.00	Total	100.00	100.00	Total	100.00	100.00
5 – layers	Elements	Weight %	Atomic %	Elements	Weight %	Atomic %	Elements	Weight %	Atomic %
	Mg	43.58	32.78	Mg	45.10	28.15	Mg	49.02	25.60
	Zn	56.42	67.22	Zn	54.90	71.85	Zn	50.98	74.40
	Total	100.00	100.00	Total	100.00	100.00	Total	100.00	100.00

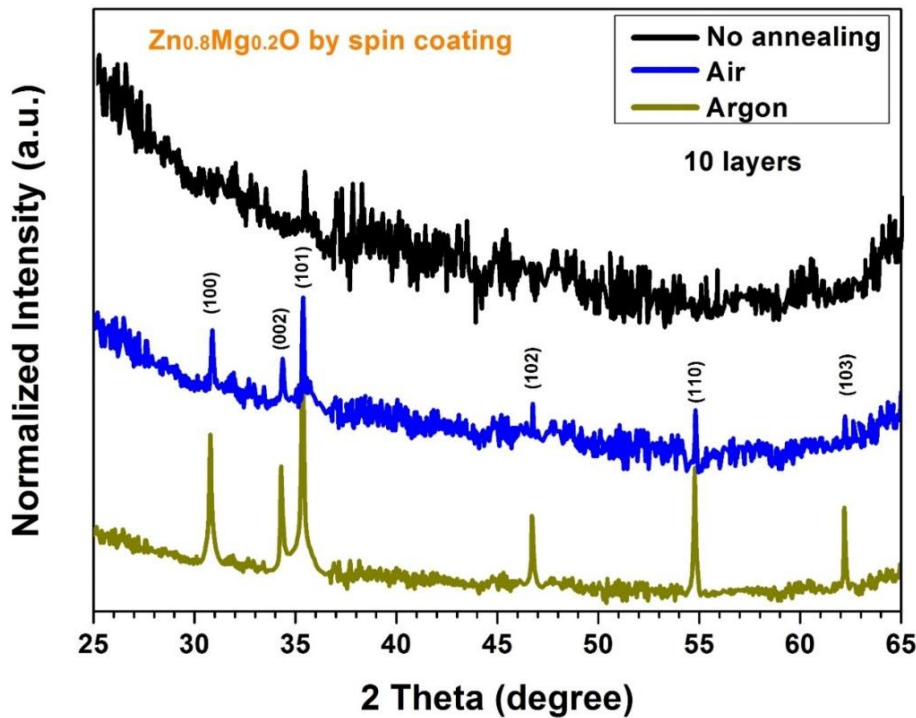

Fig. 3. X-ray diffraction pattern of $Zn_{0.8}Mg_{0.2}O/Si$ thin films (10 layers) prepared by the spin coating method and annealed in the different atmospheres.

Semiconductor oxide $(Ga_xIn_{1-x})_2O_3$ films, the band gap of which changes from 3.5 to 5 eV with a change in the alloy composition, are another material system studied in this work. Figure 4 compares the XRD patterns of $(Ga_xIn_{1-x})_2O_3$ thin films prepared by the spin coating method with a variation in the Ga concentration (x).

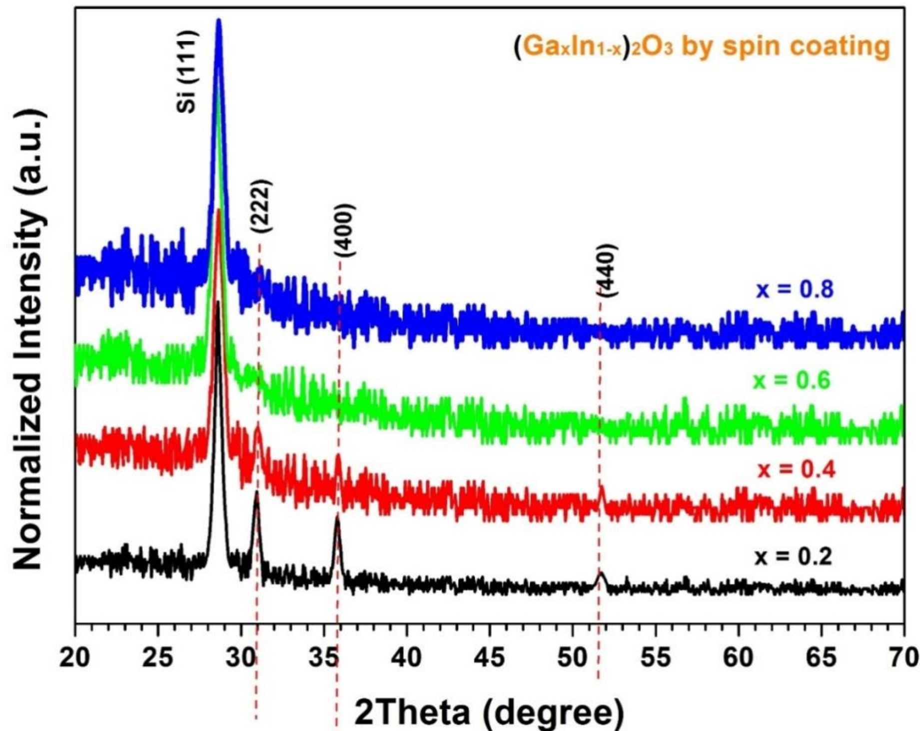

Fig. 5. X-ray diffraction pattern of $(Ga_xIn_{1-x})_2O_3$/Si thin films prepared by the spin coating method with a variation the Ga concentration (x).

The intensity of the reflections decreases with an increase in the x value up to 0.8; this fact indicates the loss of crystallinity and amorphization of the films.

Figure 4 compares the morphology of $(Ga_xIn_{1-x})_2O_3$ thin films prepared by the spin coating method with a variation in the Ga concentration (x).

The SEM images suggest that the thin film with $In_{0.8}Ga_{0.2}O$ composition are formed from small nanograins. However, the morphology evolves to amorphous formations with increasing the Ga content in films, which become more evident for the film with $In_{0.2}Ga_{0.8}O$ compostion. This siggestion is also corroboratoed by the results of the XRD analysis as discussed above.

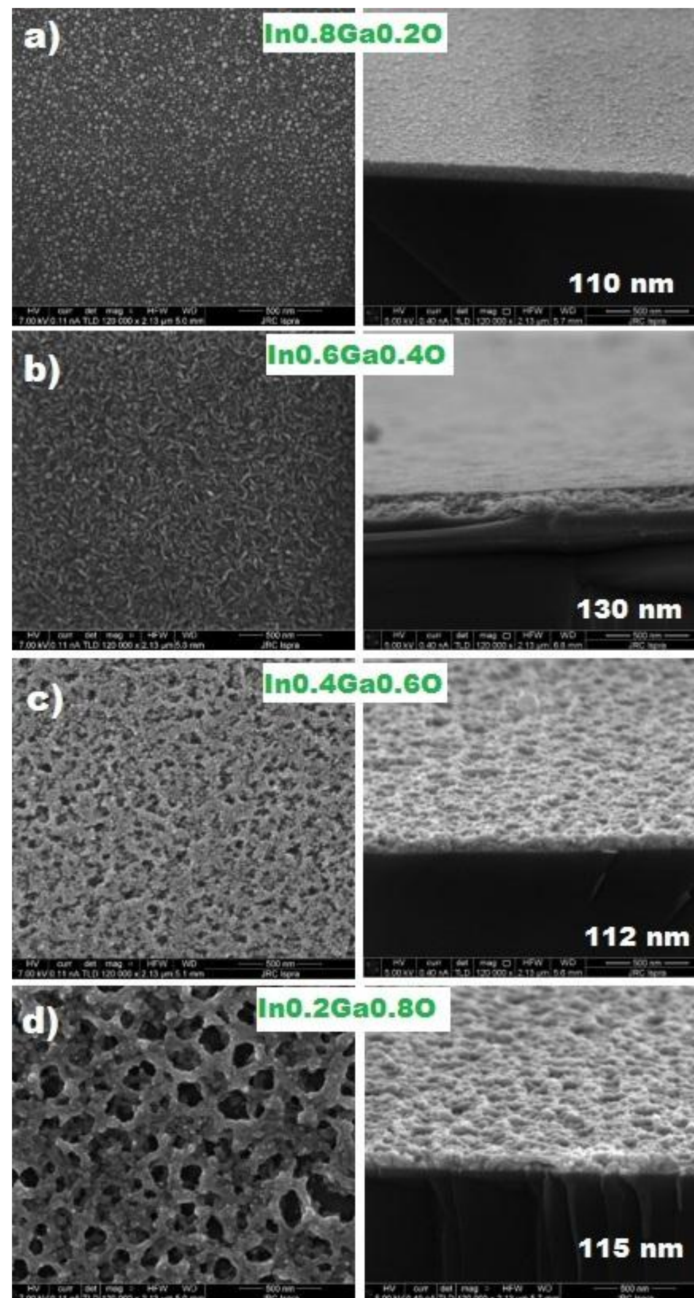

Fig. 4. Scanning electron microscopy images: top view (left column) and cross section view (right column) of $(Ga_xIn_{1-x})_2O_3$/Si thin films prepared by the spin coating method with a variation in the Ga concentration (x).

Table 2 shows results of EDX analysis of $(Ga_xIn_{1-x})_2O_3$ thin films with a variation in the Ga concentration (x). The quantitative EDX analysis suggests that a deficiency of Ga is characteristic of all the films.

Table 2. Results of EDX analysis of $(Ga_xIn_{1-x})_2O_3$ thin films prepared by the spin coating method

$In_{0.8}Ga_{0.2}O$			$In_{0.6}Ga_{0.4}O$		
Elements	**Weight %**	**Atomic %**	**Elements**	**Weight %**	**Atomic %**
Ga	14.69	**17.08**	**Ga**	27.43	**31.36**
In	85.31	**82.92**	**In**	72.57	**68.64**
Total	**100.00**	**100.00**	**Total**	**100.00**	**100.00**

$In_{0.4}Ga_{0.6}O$			$In_{0.2}Ga_{0.8}O$		
Elements	**Weight %**	**Atomic %**	**Elements**	**Weight %**	**Atomic %**
Ga	42.58	**47.43**	**Ga**	70.98	**61.89**
In	57.42	**52.57**	**In**	31.02	**38.11**
Total	**100.00**	**100.00**	**Total**	**100.00**	**100.00**

5. Conclusions

The obtained results show that the quality of $Zn_{1-x}Mg_xO$ and $(Ga_xIn_{1-x})_2O_3$ thin films deposited by the spin coating method on silicon substrates is significantly affected by the technological conditions of preparation. Annealing atmosphere is extremely important for obtaining ZnMgO films with a high-quality crystalline structure. To prepare high-quality films, it is desirable that annealing should be performed in an argon atmosphere at a temperature of 500°C. The concentration of precursor solutions for the preparation of GaInO films also significantly affects the morphology and crystalline structure of the material. With an increase in the Ga content, the films become amorphous and the morphology changes considerably. To prepare GaInO films with a stoichiometric composition, it is necessary to provide the presence of excess Ga in the precursor solutions.

Acknowledgments. This work was financially supported by the National Agency for Research and Development of the Republic of Moldova under the grants #20.80009.5007.02 “Advanced Nanostructured Materials for Thermoelectric and Sensor Applications” and by the Horizon-2020 research and innovation programme of the European Union (grant no. 810652, NanoMedTwin project).

References

[1] M. Karmaoui, A. B. Jorge, P. F. McMillan, A. E. Aliev, R. C. Pullar, J. A. Labrincha, and D. M. Tobaldi, ACS Omega 3 (10), 13227 (2018). https://doi:10.1021/acsomega.8b02122

[2] O. Mounkachi, E. Salmani, M. Lakhal, H. Ez-Zahraouy, M. Hamedoun, M. Benaissa, and A. Benyoussef, Sol. Energy Mater. Sol. Cells 148, 34 (2016). https://doi:10.1016/j.solmat.2015.09.062

[3] M. Thirumoorthi and J. Thomas Joseph Prakash, J. Asian Ceram. Soc. 4 (1), 124 (2016). https://doi:10.1016/j.jascer.2016.01.001

[4] H. Qiu, C. Cao, and H. Zhu, Mater. Sci. Eng. B 136 (1), 33 (2007). https://doi:10.1016/j.mseb.2006.08.062
[5] V. Morari, E. V. Rusu, V. V. Ursaki, K. Nielsch, and I. M. Tiginyanu. IFMBE Proc., Springer Nature Switzerland AG 87, 32 (2022). https://doi.org/10.1007/978-3-030-92328-0_5
[6] V. Morari, E. V. Rusu, V. Postolache, V. V. Ursaki, I. M. Tiginyanu, A. V. Rogachev, and A. V. Semchenko, Rom. J. Phys. 66 (7–8), Article no. 609, 1 (2021). ONLINE: ISSN 1221-146X.
[7] V. Morari, A. Pantazi, N. Curmei, V. Postolache, E. V. Rusu, M. Enachescu, I. M. Tighineanu, and V. V. Ursaki, Beilstein J. Nanotechnol. 11, 899 (2020). https://doi.org/10.3762/bjnano.11.75
[8] V. Morari, V. Postolache, G. Mihai, E. Rusu, Ed. Monaico, V. V. Ursachi, K. Nielsch, and I. M. Tiginyanu, IFMBE Proc., Springer 77, 105 (2020). Print ISSN 1680-0737, Online 1433-9277. https://doi.org/10.1007/978-3-030-31866-6
[9] H.-Y. Lee, W.-H.Tsai, and Y.-C. Lin, J. Vac. Sci. Technol. B 34, 051207 (2016).
[10] J. S. Wrench, I. F. Brunell, P. R. Chalker, J. D. Jin, and A. Shaw, Appl. Phys. Lett. 105, 202109 (2014).
[11] Y. N. Hou, Z. X. Mei, H. L. Liang, D. Q. Ye,and C. Z. Gu, Appl. Phys. Lett. 102, 153510 (2013).
[12] M. M. Morshed, M. Suja, Z. Zuo, and J. Liu, Appl. Phys. Lett. 105, 211107 (2014).
[13] S. Choopun, R. D. Vispute, W. Yang, R. P. Sharma, and T. Venkatesan, Appl. Phys. Lett. 80, 1529 (2002).
[14] X. Wang, K. Saito,T. Tanaka, M. Nishio, and Q. Guo, J. Alloys Compd. 627, 383 (2015).
[15] J.-S. Shiau, S. Brahma, C.-P. Liu,and J.-L.Huang, Thin Solid Films 620, 170 (2016).
[16] Y. G. Kim, T. Kim, C. Avis, S.-H. Lee, and J. Jang, IEEE Trans. Electron Devices 63, 1078 (2016).
[17] G. Gonçalves, P. Barquinha, L. Pereira, N. Franco, E. Alves, et al., Electrochem. Solid-State Lett. 13, H20 (2010).
[18] S. I. Stepanov, V. I. Nikolaev, V. E. Bougrov, and A. E. Romanov, Rev. Adv. Mater. Sci. 44, 63 (2016).
[19] W.-L. Huang, M.-H. Hsu, S.-P. Chang, S.-J. Chang, and Y.-Z. Chiou, ECS J. Solid State Sci. Technol. 8, Q3140 (2019).
[20] S. J. Pearton, J. Yang, P. H. Cary, F. Ren, J. Kim, M. J. Tadjer, and M. A. Mastro, Appl. Phys. Rev. 5, 011301 (2018). https://doi.org/10.1063/1.5006941
[21] C. Y. Wang, I. Kirste, F. M. Morales, J. M. Mánuel, et al., J. Appl. Phys. 110 (9), 093712 (2011). https://doi:10.1063/1.3658217
[22] S. Stepanov, V. Nikolaev, A. Pechnikov, M. Scheglov, A. Chikiryaka, A. Chernykh, and A. Y. Polyakov, Phys. Status Solidi A, 218 (3), 2000442 (2020). https://doi:10.1002/pssa.202000442
[23] E. J. Tarsa, J. H. English, J. S. Speck, et al., Appl. Phys. Lett. 62 (19), 2332 (1993). https://doi:10.1063/1.109408
[24] A. Papadogianni, T. Nagata, and O. Bierwagen, Jpn. J. Appl. Phys. 61, 045502 (2022). https://doi.org/10.35848/1347-4065/ac4ec7
[25] V. Morari, V. Postolache, E. Rusu, K. Leistner, K. Nielsch, V. V. Ursaki, and I. M. Tiginyanu, Int. Conf. ATOM-N 2022, 11th edition, August 20–23, Contanta, Romania, Proc. SPIE-Int. Soc. Opt. Eng., Bellingham, USA, vol. 11718, 2020. https://doi.org/10.1117/12.2571189